Geophysical Research Letters

Supporting Information for

Atmospheric circulation constraints on 21st century seasonal precipitation storylines for the southwestern United States

Kevin M. Grise[1]

[1] Department of Environmental Sciences, University of Virginia, Charlottesville, VA, USA

Contents of this file

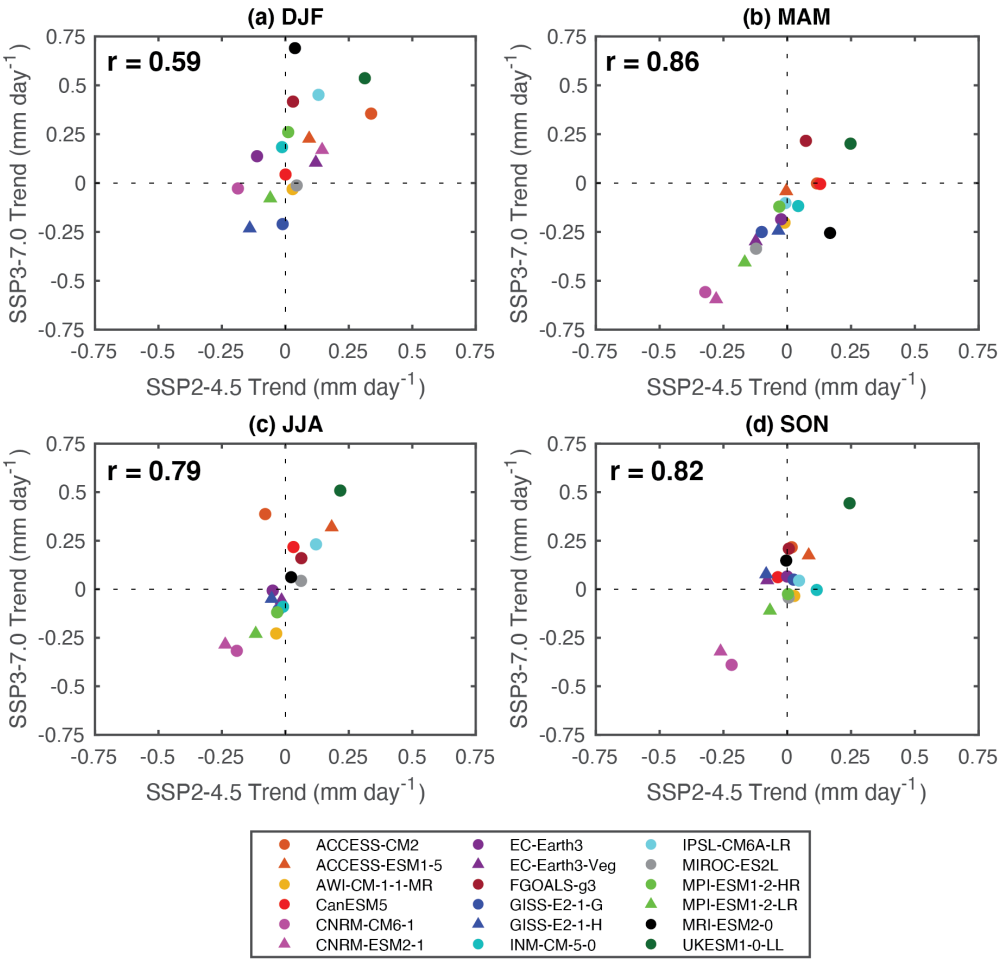

Figure S1. Scatter plots between model-mean 2015–2100 precipitation trends (mm day^{-1} change over 86 years) for the SSP2-4.5 and SSP3-7.0 scenarios. The model mean reflects the average over all ensemble members for each model for the SSP3-7.0 scenario (as listed in Table S1) and the mean over all available corresponding ensemble members for the SSP2-4.5 scenario.

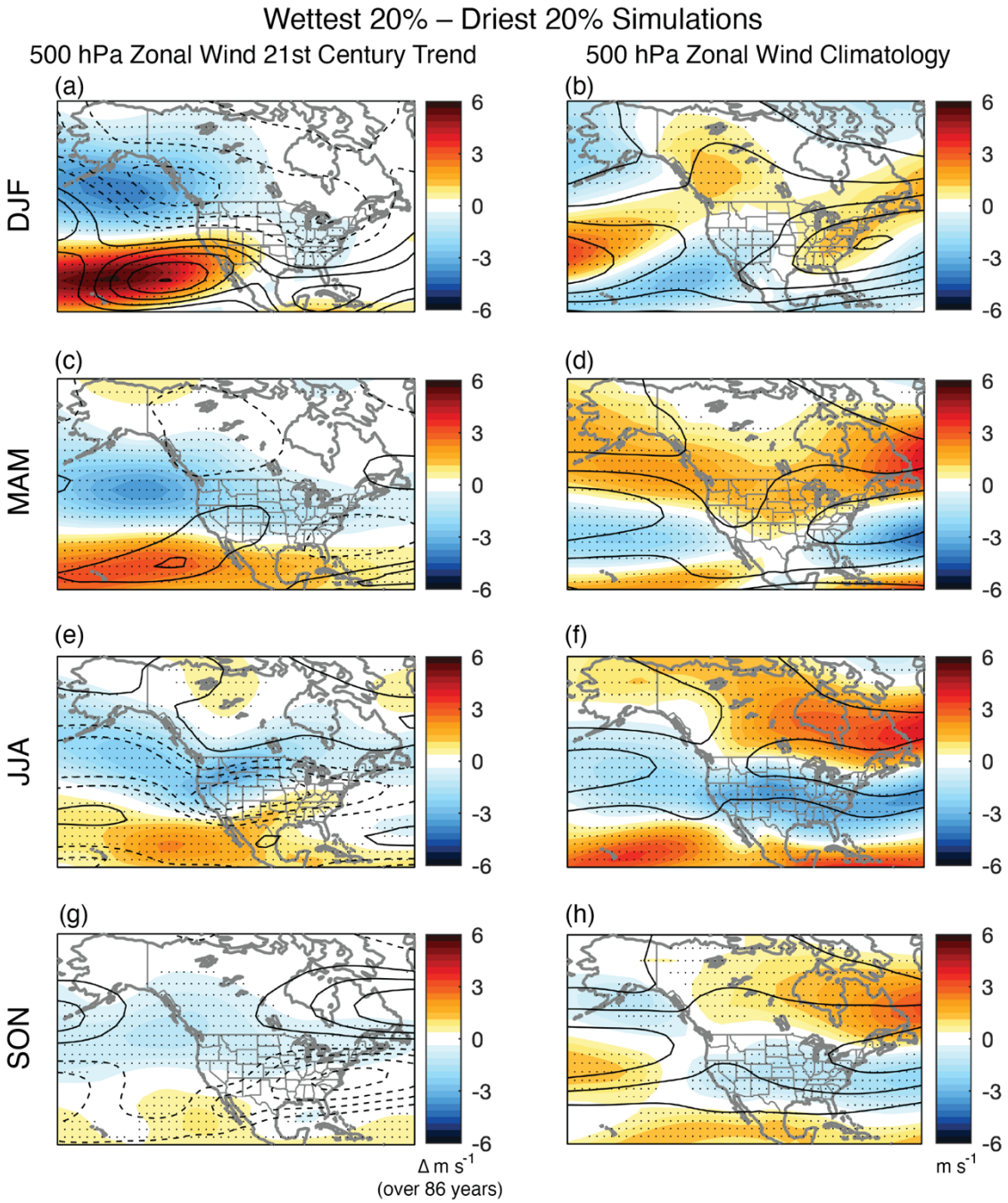

Figure S2. As in Fig. 2, but for the 500 hPa zonal wind field. Thin solid lines indicate multi-model mean (left column) trend (contour interval: 0.5 m s^{-1} change over 86 years) and (right column) climatology (contour interval: 5 m s^{-1}), with dashed contours denoting negative values. Note that here the composites in the right column are based on the 2015–2044 climatology (i.e., the first 30 years of the SSP3-7.0 scenario) instead of the 1992–2021 climatology. As shown in Fig. S8, results are virtually identical if either the 1992–2021 or 2015–2044 periods are used to define the climatology for these composites.

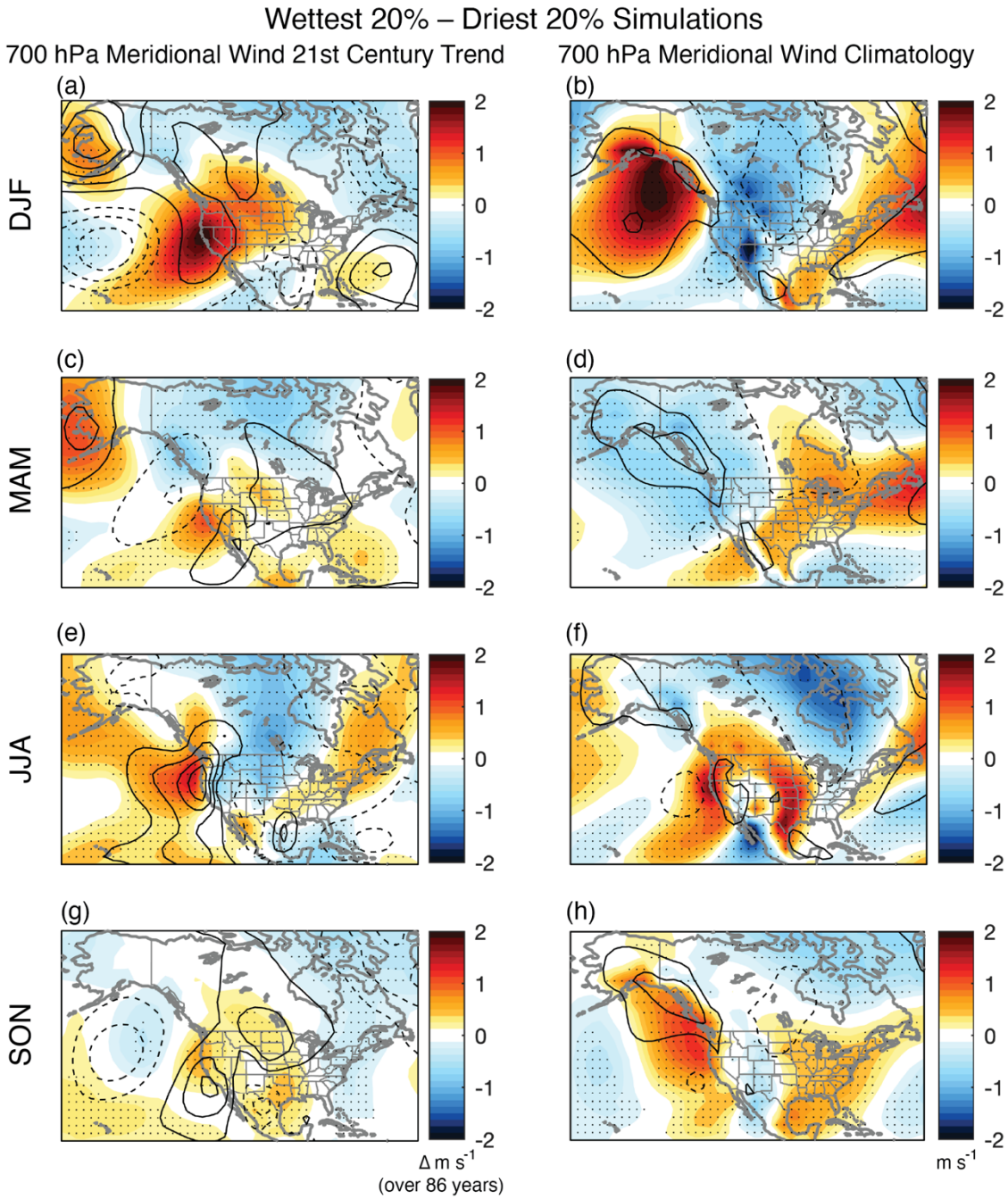

Figure S3. As in Fig. S2, but for the 700 hPa meridional wind field. Thin solid lines indicate multi-model mean (left column) trend (contour interval: 0.25 m s^{-1} change over 86 years) and (right column) climatology (contour interval: 2 m s^{-1}), with dashed contours denoting negative values.

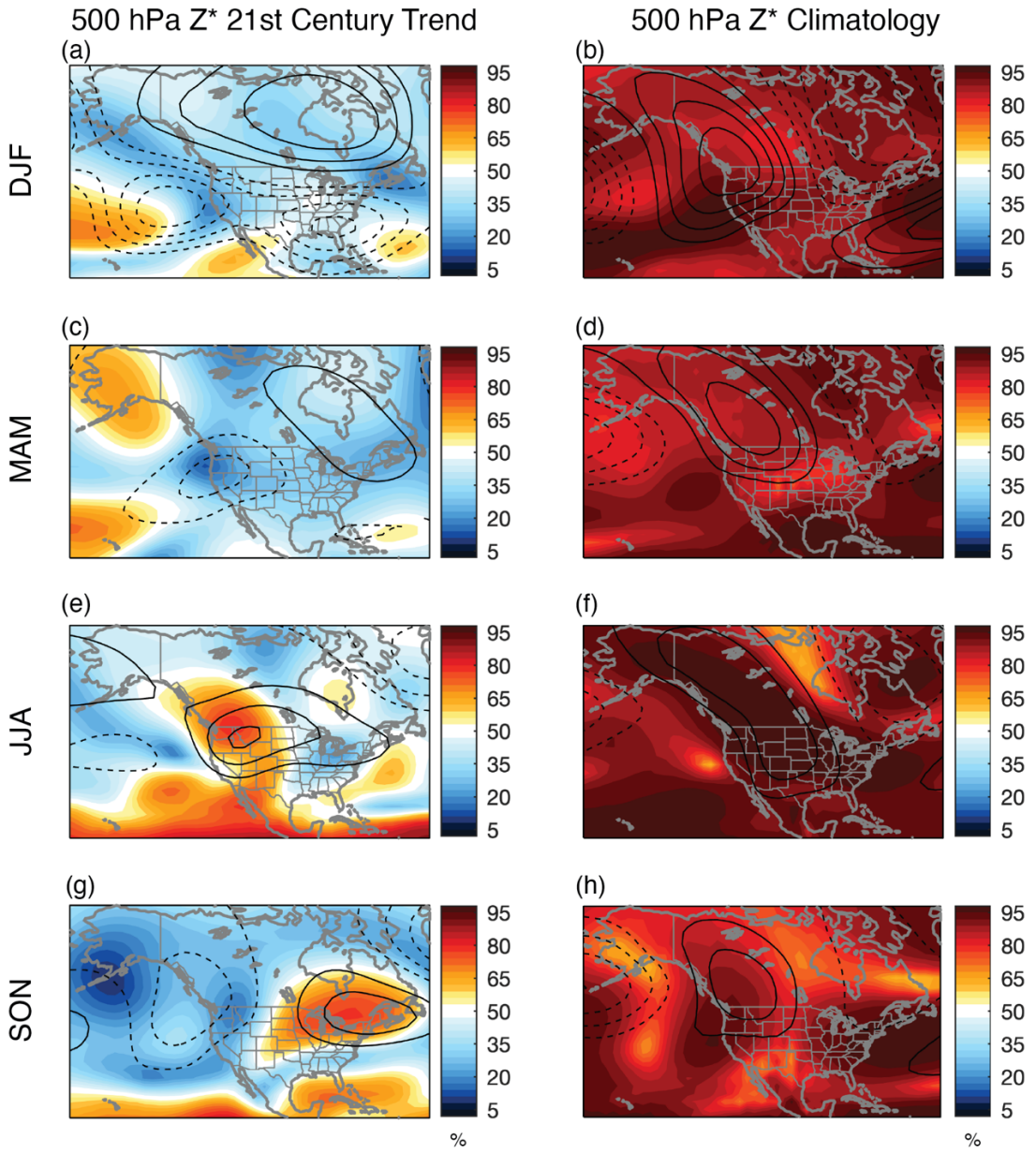

Figure S4. Percent variance explained by model-to-model differences for (left column) 2015–2100 500 hPa *Z** trends and (right column) 1992–2021 500 hPa *Z** climatology among 248 CMIP6 simulations. The red shading indicates that the variance among simulations is dominated by inter-model differences, and the blue shading indicates that the variance among simulations is dominated by intra-model differences (internal variability). As in Fig. 2, thin solid lines indicate multi-model mean (left column) trend (contour interval: 5 m change over 86 years) and (right column) climatology (contour interval: 20 m), with dashed contours denoting negative values.

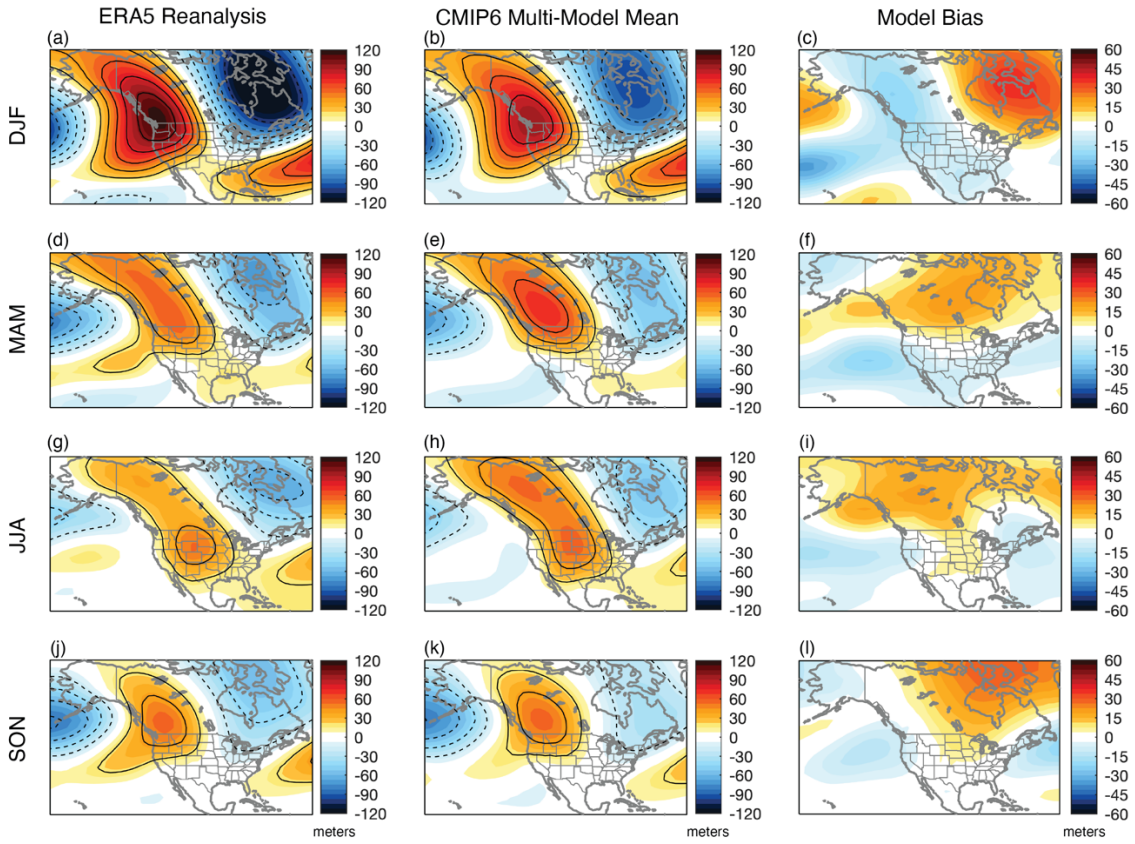

Figure S5. 1992–2021 500 hPa *Z** climatology for (left column) ERA5 reanalysis, (middle column) CMIP6 multi-model mean (historical + SSP3-7.0 scenarios), and (right column) difference (CMIP6 – observations). As in the right column of Fig. 2, thin solid lines in the first two columns highlight contours at intervals of 20 m, with dashed lines denoting negative contours.

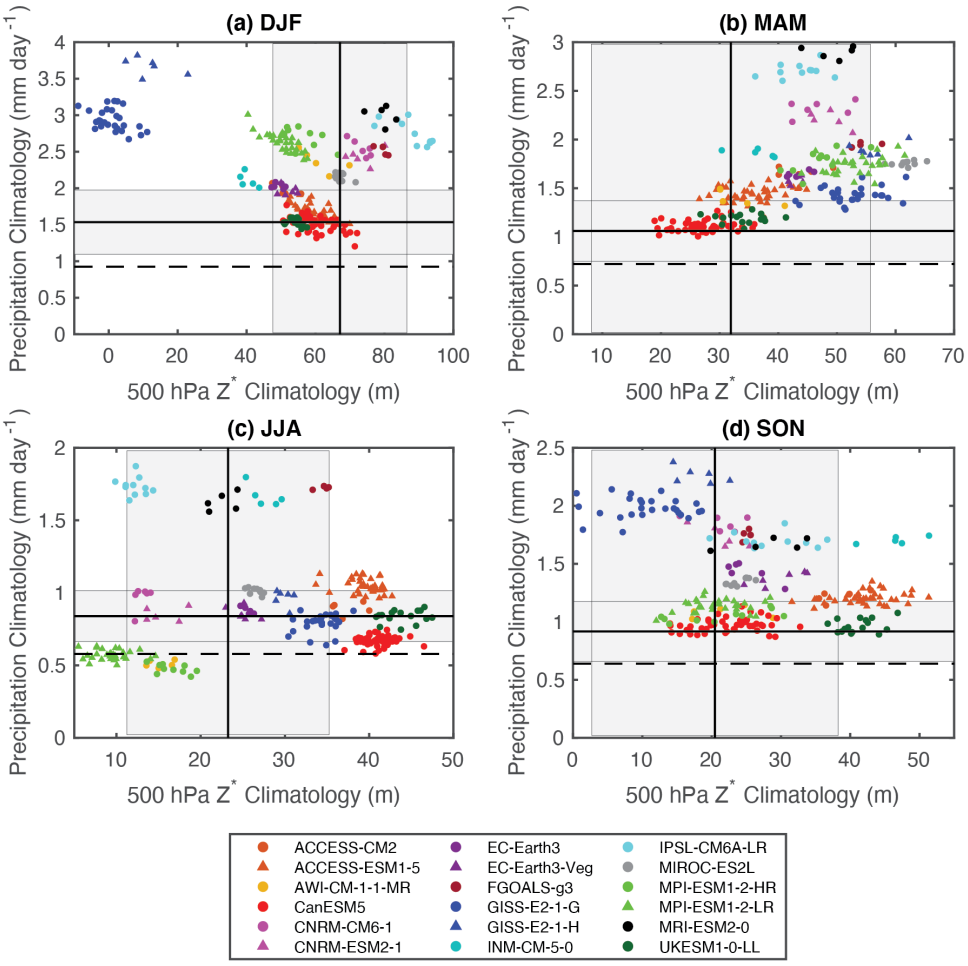

Figure S6. Scatter plots between 1992–2021 500 hPa *Z** climatology within the boxed regions shown in Fig. 2 and 1992–2021 precipitation climatology for the southwestern United States for 248 CMIP6 model simulations. The solid vertical line indicates the 1992–2021 500 hPa *Z** climatology from the ERA5 reanalysis, the solid horizontal line indicates the 1992–2021 precipitation climatology from the Global Precipitation Climatology Project (GPCP) data set (Adler et al., 2003), and the dashed horizontal line indicates the 1992–2021 precipitation climatology from the CPC Merged Analysis of Precipitation (CMAP) data set (Xie & Arkin, 1997). Light gray shading indicates the one standard deviation bounds on the ERA5 and GPCP means.

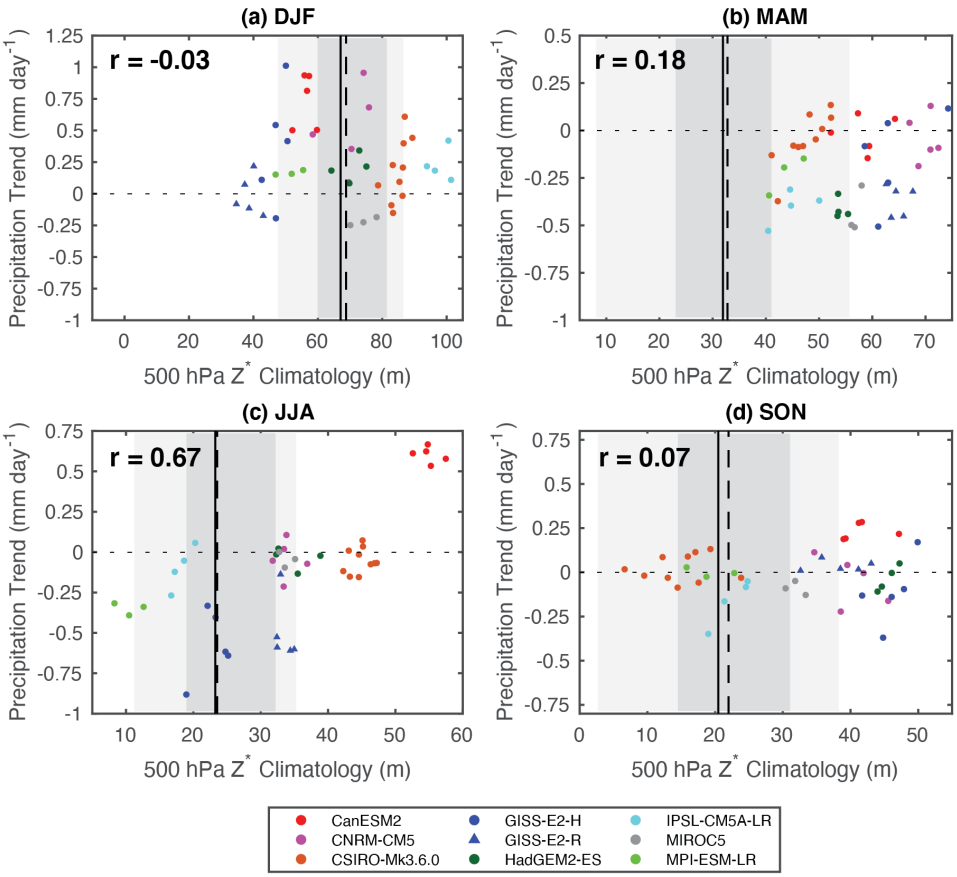

Figure S7. As in Fig. 3, for CMIP5 models (Taylor et al., 2012) with at least 3 ensemble members available for the Representative Concentration Pathway (RCP) 8.5 scenario. Note that, for the DJF and MAM seasons, CMIP5 models do not sample the full range of values of the 500 hPa *Z** climatology seen in CMIP6 models.

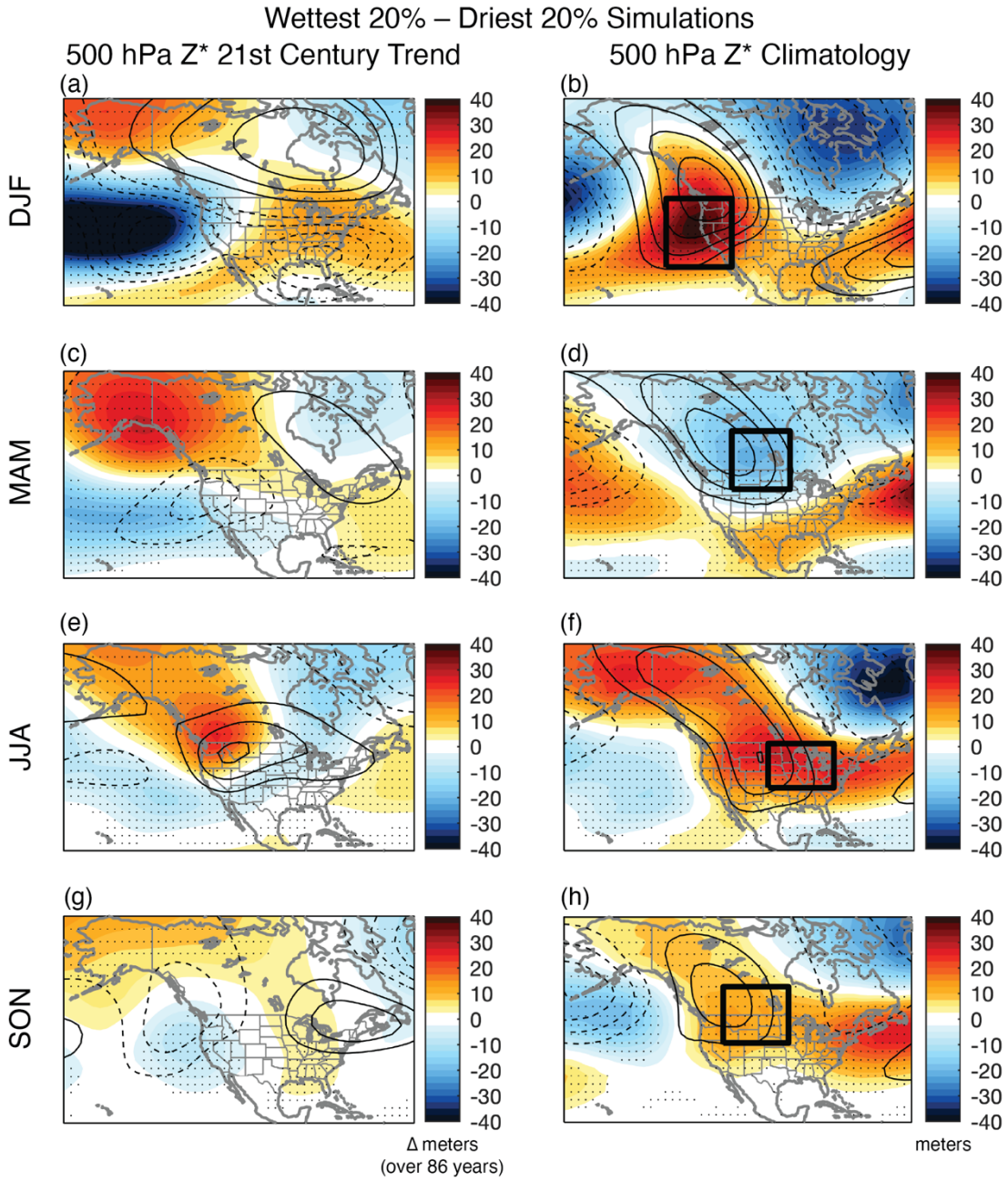

Figure S8. As in Fig. 2, but with the composites in the right column based on the 2015–2044 500 hPa *Z** climatology (i.e., the first 30 years of the SSP3-7.0 scenario) instead of the 1992–2021 500 hPa *Z** climatology.

CMIP6 Model	Number of Ensemble Members	Dataset Reference
ACCESS-CM2	5	Dix et al. (2019)
ACCESS-ESM1-5	40	Ziehn et al. (2019)
AWI-CM-1-1-MR	5	Semmler et al. (2019)
CNRM-CM6-1	6	Voldoire (2019)
CNRM-ESM2-1	5	Seferian (2019)
CanESM5	50	Swart et al. (2019)
EC-Earth3	6	EC-Earth (2019a)
EC-Earth3-Veg	6	EC-Earth (2019b)
FGOALS-g3	5	Li (2019)
GISS-E2-1-G	27	NASA/GISS (2020a)
GISS-E2-1-H	6	NASA/GISS (2020b)
INM-CM-5-0	5	Volodin et al. (2019)
IPSL-CM6A-LR	11	Boucher et al. (2019)
MIROC-ES2L	10	Tachiiri et al. (2019)
MPI-ESM1-2-HR	10	Schupfner et al. (2019)
MPI-ESM1-2-LR	30	Wieners et al. (2019)
MRI-ESM2-0	5	Yukimoto et al. (2019)
UKESM1-0-LL	16	Good et al. (2019)

Table S1. Listing of CMIP6 models used in this study.